Hindawi Publishing Corporation
Journal of Nanomaterials
Volume 2015, Article ID 458629, 7 pages
http://dx.doi.org/10.1155/2015/458629

Research Article

In-Channel-Grown Polypyrrole Nanowire for the Detection of DNA Hybridization in an Electrochemical Microfluidic Biosensor

Thi Luyen Tran,[1] Thi Xuan Chu,[1] Phuc Quan Do,[2] Duc Thanh Pham,[1] Van Vu Quan Trieu,[1] Dang Chinh Huynh,[1] and Anh Tuan Mai[1]

[1]*Hanoi University of Science and Technology, No. 1, Dai Co Viet Road, Hanoi 100000, Vietnam*
[2]*University of Science, Vietnam National University (Hanoi), 334 Nguyen Trai Road, Hanoi 100000, Vietnam*

Correspondence should be addressed to Thi Xuan Chu; xuan@itims.edu.vn and Anh Tuan Mai; tuan.maianh@hust.edu.vn

Received 17 June 2015; Revised 10 August 2015; Accepted 31 August 2015

Academic Editor: Matteo Tonezzer

A triple electrode setup with a Pt pseudo-reference electrode integrated in a polydimethylsiloxane- (PDMS-) based microchamber was designed and fabricated. The integrated electrodes were deposited onto SiO_2/Si substrate by sputtering. The PDMS microchamber was patterned using an SU-8 mold and sealed with electrodes in oxygen plasma. Polypyrrole nanowires (PPy NWs) were electrochemically grown in situ at an accurate position of the working electrode in the sealed microchamber instead of in an open system. The DNA probe sequences were simply introduced into the channel to form bonds with the nanowires. A detection limit of 20 pM was achieved using a lock-in amplifier. The electrochemical characteristics produced by the hybridization of DNA strands in the microchamber showed a good signal/noise ratio and high sensitivity. Measurement of the DNA sensor in narrow space also required much less volume of the analytical sample compared with that in an open measuring cell. Results showed that this simple system can potentially fabricate nanostructures and detect bio/chemical molecules in a sealed system.

1. Introduction

In the 1990s, microfluidics emerged as a powerful technology and is now widely used in many fields, such as chemistry, biology, and biomedicine [1]. The combination of microfluidic technique and biosensors has attracted increasing attention [2–4] because of its many advantages, including small sample consumption, fast analysis, high sensitivity, and portability. The development of microfluidics integrated with biosensors is also considered a stepping stone for future lab-on-chip device. Instead of carrying out individual steps, all steps are combined in a small handy kit consisting of a number of components, such as pumps, chamber, mixing chamber, and controllable valves [5, 6]. Almost all manipulations have occurred within the system, including preparation of reagents, reaction, detection, data acquisition, and treatment [7, 8]. The combined microfluidic technique and biosensor not only develop the analytical ability and results but also broaden the perspective of possible application.

In this study, electrochemical sensors were used because of high precision and integration ability [2, 9–12]. The sensor consists of working, counter, and reference electrodes. Given that these electrodes are integrated in the microchamber, the replacement of the conventional reference electrode by a pseudo-reference electrode (PRE) facilitates the miniaturization of the analytical system. The microfluidic biosensor integrated PRE has been used in many studies for the determination of medicament [13], cell morphological changes [12], heavy metals [14], and glucose [2] in aqueous solution. However, little research has been dedicated to the synthesis of nanostructures inside the integrated three-electrode chip.

Nowadays, one-dimensional nanoscale structures, such as rod, tube, and wire, become indispensable for microfluidic devices because of their unique properties at micro- and nanoscales [11, 15]. The fabrication of nanostructures at accurate position inside the packed devices is also very important for bioelement immobilization and detection. The conducting polymers, such as PPy, polyaniline, and polythiophene,

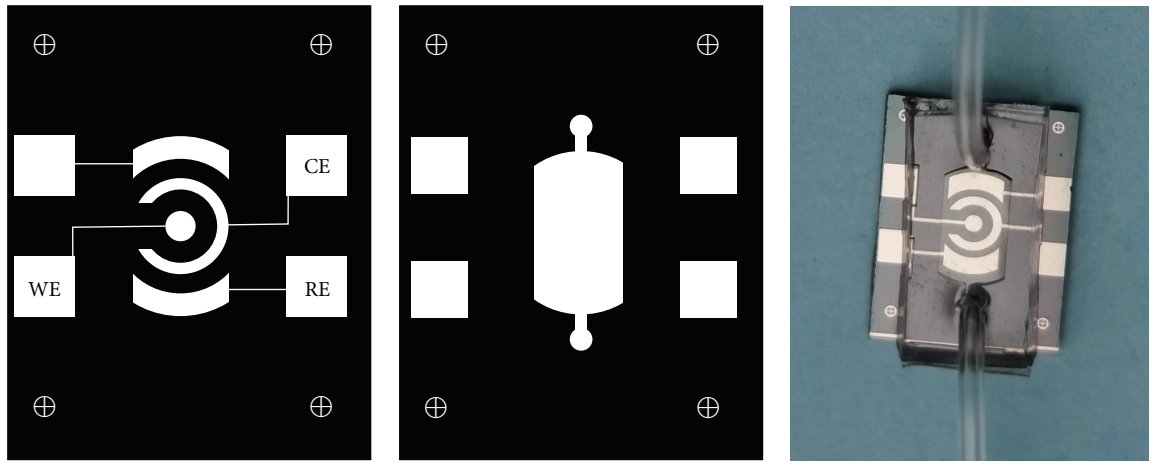

(a) (b) (c)

Figure 1: (a) The mask for Pt electrode fabrication (Mask 1) and (b) for SU-8 mold (Mask 2); (c) the integrated three-electrode sensor using Pt pseudo-reference electrode in the microchamber. The size of the chip: 12 × 15 mm.

play an important role in immobilizing bioelements to enhance the sensitivity and stability of the electrochemical biosensors [16, 17]; PPy is one of the most popular polymers because of its good electrical conductivity, ease of preparation, and chemical stability [18, 19]. Recent works [20, 21] reported the synthesis of PPy NWs in an open system. PPy NWs facilitate the immobilization of biorecognition on the sensor's surface and increase the sensitivity of the sensor compared with the PPy bulk film [22].

The present work aims to study the growth of PPy NWs in microchamber. We hypothesize that the nanostructure of polypyrrole, microchamber, and triple-electrode integration may improve the biosensor's characteristics.

2. Materials and Methods

2.1. Chemicals. SU-8 3050 and PDMS Sylgard 184 were obtained from Microchem and Dow Corning, respectively. Meanwhile, pyrrole (99.9%) and phosphate buffer solution (PBS) were purchased from Merck. The supporting chemicals $LiClO_4 \cdot 3H_2O$, gelatin, KCl, $K_2Cr_2O_7$ (99%), H_2SO_4 (98%), N_2 (99.9%), $K_3Fe(CN)_6$, and $K_4Fe(CN)_6$ are of analytical grade. ssDNA were obtained from Sigma Aldrich.

The ssDNA probe and the complementary and noncomplementary target are as follows:

Probe: thiol-C_6-5′-AGACCTCCAGTCTCCATGGTACGTC-3′.

Complementary target: 5′-GACGTACCATGGAGACTGGAGGTCT-3′.

Noncomplementary target: 5′-ACGCTGAGTACGGGTGCAAGAGTCA-3′.

2.2. Integrated Three-Electrode Setup Using Pt PRE Associated with the Microchamber

Fabrication of the Three-Electrode Setup. The integrated Pt electrode consists of a round working electrode with 0.8 mm^2 area, a 5 mm^2 counter electrode, and a reference electrode (Figure 1(a)). These electrodes were deposited on SiO_2/Si substrate by cathode sputtering technique. The fabrication process was previously discussed in detail [20].

Fabrication of the Microchamber. The SU-8 mold was prepared by using a conventional photolithography technique (Figure 1(b)). After cleaning with $K_2Cr_2O_7$, the silicon wafer was deposited with 250 μm thick SU-8 3050 using simple spin coating at 500 rpm for 60 s [25]. By applying Mask 2, the wafer was exposed to the UV light (250 W, 12 mW/cm) for 30 s. The development was followed by the immersion of wafer in a sonicated 1-ethoxy-2-propyl acetate solution for 7 min to remove the unexposed parts. Finally, the wafer was rinsed with deionized water and blown dry with nitrogen. The SU-8 on the wafer was defined as the mold for the next step. The microchamber was first formed by locating the mold in a plastic Petri dish. Subsequently, the PDMS prepolymer and curing agent solution (10 : 1 in volume) were poured into the dish. The mixture was degassed in a vacuum desiccator and solidified at 70°C in 2 h.

Bonding of Microchamber and Electrodes. The electrodes were bonded with the PDMS microchamber in oxygen plasma (10 Pa and 20 W for 20 s, Figure 1(c)). Sealing was stabilized by further heat treatment in 15 min at 70°C and cooled down to room temperature.

2.3. Electrochemical Synthesis of PPy NWs inside the Microchamber. The PPy NWs were synthesized using the PGSTAT30 AutoLab electrochemical workstation (Eco Chemie, Netherlands) inside the sealed system fabricated above. Before the experiment, the electrode system was cleaned in a saturated solution of $K_2Cr_2O_7/H_2SO_4$ and electrochemically activated in 0.5 M H_2SO_4 solution by sweeping the voltage from −0.5 V to 1 V until the cyclic voltammetry characteristics were stable. Electrolyte solution, which is composed of 0.1 M pyrrole monomer, 0.08%

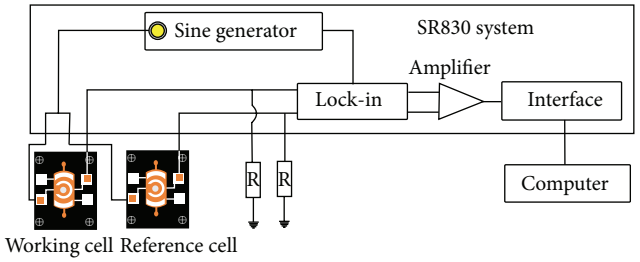

FIGURE 2: The differential measurement setup using SR830 DSP lock-in amplifier.

gelatin in weight, 0.1 M $LiClO_4$, and PBS buffer (pH = 7.4), was pumped into the microchamber. To purge the dissolved oxygen in the electrolyte, N_2 gas was blown into the chamber for 15 min. Polymerization was conducted at room temperature for 1200 seconds. The applying polarized voltage was set at 0.5 V.

The surface morphology of the working electrode was investigated using Hitachi S4800 Scanning Electron Microscope (SEM). Meanwhile, the structure of the obtained PPy NWs was investigated using Thermo Nicolet 6700 Fourier Transform Infrared (FTIR) spectroscopy. Cyclic voltammograms (CV) measurements were performed in 0.03 M $K_3Fe(CN)_6/K_4Fe(CN)_6$ and 0.1 M KCl solution at 25 mV/s scan rate to investigate the electrochemical behavior of the integrated three-electrode system inside the microchamber. Electrochemical impedance spectroscopy (EIS) measurements of PPy NWs/Pt electrodes were performed within the frequency range of $5{\cdot}10^4$–0.05 Hz at an applied DC potential and amplitude of 50 and ±5 mV, respectively, in an electrolyte solution containing 0.03 M $K_3Fe(CN)_6/K_4Fe(CN)_6$ and 0.1 M KCl in the microchamber.

2.4. Probe DNA Immobilization on the PPy NWs/Pt Electrodes. DNA probe sequences were immobilized on the PPy NWs/Pt electrode using the adsorption method. A volume of 4 μL of 10 μM probe DNA solution was pumped into the electrode-integrated microchamber for 2 h. The system was cleaned by deionized water to remove the unspecific probe DNA molecules, which did not bind or have weak linkage with PPy NWs. The DNA electrodes were dried and prepared for further measurements.

2.5. DNA Hybridization Detection Using Lock-In Amplifier. The measurement of DNA hybridization was performed at room temperature by using SR830 DSP lock-in amplifier from the Stanford Research (Figure 2). The lock-in amplifiers are used to detect and measure very small AC signals, down to a few nanovolts. The SR830 generates its own sine wave, named reference signal, which has a frequency and amplitude of 10 kHz and 100 mV, respectively. This reference signal was then set on two identical electrodes of two different systems for excitation and amplification. The surface of one electrode was immobilized with the probe DNA/PPy nanowires (as working electrode), and the surface of the remaining electrode was modified using PPy nanowires only (as reference electrode). When about 4 μL of the solution containing the complementary target DNA was pumped into the microchamber, DNA hybridization occurred on the working electrode (with the immobilized probe DNA), and thus the change in the charges of the conducting membrane and thereby the output signal compared with that in reference electrode (without the immobilized probe DNA) as the final output signal.

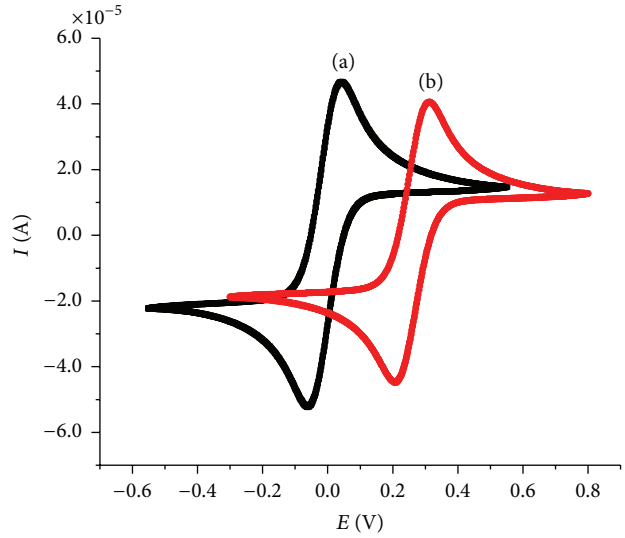

FIGURE 3: Cyclic voltammograms measured in 0.03 M $K_3Fe(CN)_6/K_4Fe(CN)_6$ and 0.1 M KCl solution at 25 mV/s scan rate of (a) integrated three-electrode system inside the microchamber using Pt electrode as pseudo-reference electrode and (b) three-electrode system using Ag/AgCl (in saturated KCl) reference electrode in the open cell.

3. Results and Discussion

3.1. Electrochemical Behavior of the Integrated Three-Electrode System in the Microchamber. Figure 3 shows the CV of the three-electrode system inside the microchamber using Pt electrode as pseudo-reference electrode (Figure 3(a)) and in the open cell using Ag/AgCl (in saturated KCl) conventional reference electrode (Figure 3(b)), measured in 0.03 M $K_3Fe(CN)_6/K_4Fe(CN)_6$ and 0.1 M KCl solution at 25 mV/s scan rate. The performance of the integrated system using the Pt pseudo-reference electrode (located inside the microchamber) was as good as that obtained in the open cell. In both cases, two peaks (0.05 V/−0.05 V and 0.31 V/0.21 V) corresponded to the oxidation of Fe^{2+} and reduction of Fe^{3+} on the CV curves, respectively. The difference between the anodic and cathodic peak potentials, ΔE, was almost unchanged after 10 CV cycles. In the microchamber, an increase in the electron transfer of the redox couple (ferro-/ferricyanide) caused the total measured current to increase to about 10% compared with the open system. The electrochemical characteristics are well stable because of the narrow, packed microchamber. The use of such microchamber can reduce the analytical volume and is expected to increase accuracy, enhance the rate of signal/noise, and contribute

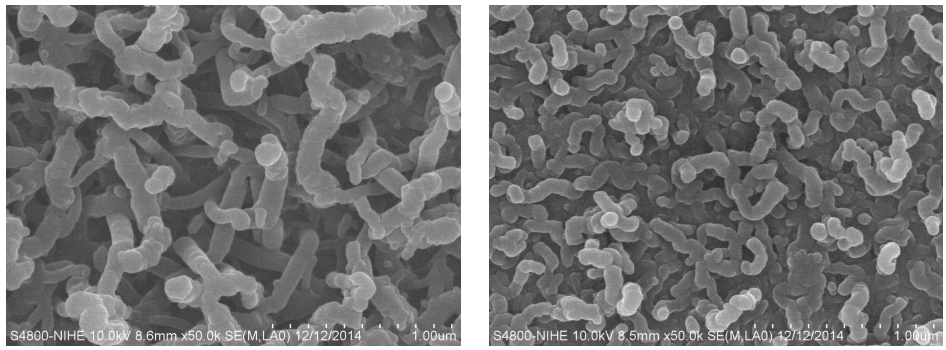

(a) (b)

Figure 4: FE-SEM images of PPy nanowires synthesized in 0.1 M Py, 0.1 M $LiClO_4$, PBS, and gelatin 0.08% wt in the microchamber by using (a) potentiostatic mode (0.5 V, 1200 s) and (b) cyclic voltammetry mode (0–0.6 V, 6 scans, 25 mV/s scan rate).

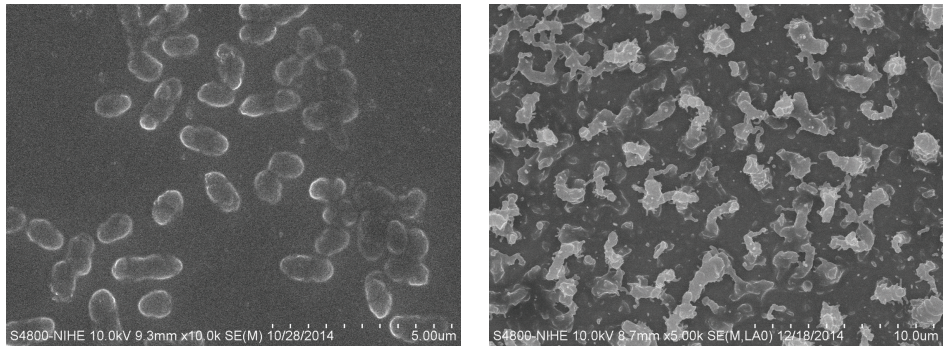

(a) (b)

Figure 5: FE-SEM images of products synthesized in 0.1 M $LiClO_4$, PBS, and gelatin 0.08% wt and (a) without Py; (b) 0.1 M Py in the microchamber by using potentiostatic mode (0.5 V, 150 s).

to improvement of the sensitivity of electrochemical sensors. These advantages make this microchamber suitable for biosensor application.

The voltage corresponding to the peak of Fe^{2+} oxidation was reduced by 0.26 V compared with the use of Ag/AgCl (in saturated KCl) as reference electrode (Figure 3). The replacement of a conventional reference electrode (normally confined in a saturated KCl solution) by a pseudo-electrode caused the shift on the potential. Fortunately, this shift in potential did not influence the final result as the data were acquired and processed in differential mode. Thus, the applied polarized voltage was set at 0.50 V for the synthesis of PPy NWs in the microchamber, instead of 0.75 V in the case of an open cell in previous works [20, 21].

3.2. Electrochemical Synthesis of PPy NWs in the Microchamber

FE-SEM Images of PPy NWs. Figure 4 shows the SEM images of PPy synthesized using potentiostatic mode (Figure 4(a)) and cyclic voltammetry mode (Figure 4(b)). When using the two electrochemical techniques, PPy NWs with 80–110 nm diameter and few micrometers long were formed on the surface of the working electrode. The size of the synthesized PPy NWs is uniform, and the nanowires are evenly distributed throughout the surface of the working electrode. Generally, the electrochemical polymerization in narrow space (4 μL in this work) without agitation caused the difficulty of growing PPy NWs. However, the isolated sealed cell could reduce the interference and influence of the surrounding environment significantly. PPy NWs were grown with high uniformity and distributed porosity that is favorable for the immobilization process of DNA through the linkages between the amino groups of PPy NWs and phosphate groups of DNA strands.

Gelatin and the Growth of PPy NWs in the Microchamber. The synthesized PPy with cauliflower structure was previously reported [20, 21]. Gelatin, as a soft mold, helped in the growth of PPy in nanowire form. To understand the role of gelatin in the polymerization process, electrochemical synthesis was performed in potentiostatic mode (0.5 V, 150 s), with 0.08 wt% gelatin but without Py monomers (Figure 5(a)) and with 0.1 M Py monomers (Figure 5(b)). In Figure 5(a), the capsule-shaped blocks of gelatin were formed with a diameter of about 1 μm. Meanwhile, in Figure 5(b), PPy NWs (D~100 nm) began to grow around the gelatin blocks. This behavior could be observed because polymerization was established in 150 s, which is the propagation phase of a polymerization reaction. The long chain structure of gelatin

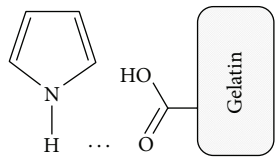

Figure 6: Hydrogen bond between pyrrole monomer and gelatin.

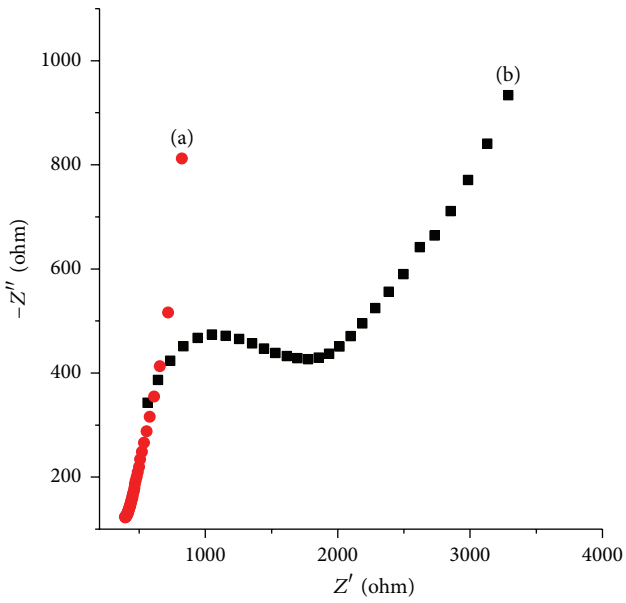

(a) Pt
(b) Pt/PPy NWs

Figure 7: Electrochemical impedance spectra of (a) Pt and (b) Pt/PPy NWs electrodes.

contains various amino acids (functioned with $-NH_2$ and –COOH groups). The –COOH group can bind with –NH group of pyrrole monomer, by means of hydrogen bond (Figure 6). Consequently, pyrrole monomers are adsorbed onto the surfaces of the gelatin chains, and polymerization continued to form PPy nanowires. Gelatin is supposed to act as the "soft template" to guide the PPy nanowire formation [26].

Electrochemical Impedance Spectra of Pt and Pt/PPy NW Electrodes. Figure 7 shows electrochemical impedance spectra in the Nyquist form of Pt and Pt/PPy NW electrodes; EIS was performed in the frequency range of $5{\cdot}10^4$–0.05 Hz at an applied DC potential and amplitude of 50 and ±5 mV, respectively, in the electrolyte solution containing 0.03 M $K_3Fe(CN)_6/K_4Fe(CN)_6$ and 0.1 M KCl. Generally, the impedance is represented by

$$Z_{(\omega)} = Z_{re} - jZ_{im}, \quad (1)$$

where Z_{re} and Z_{im} are the real and imaginary parts of the impedance, respectively. Unlike the electrochemical impedance of Pt electrode, the electrochemical impedance spectrum of Pt/PPy NW electrode consists of two parts:

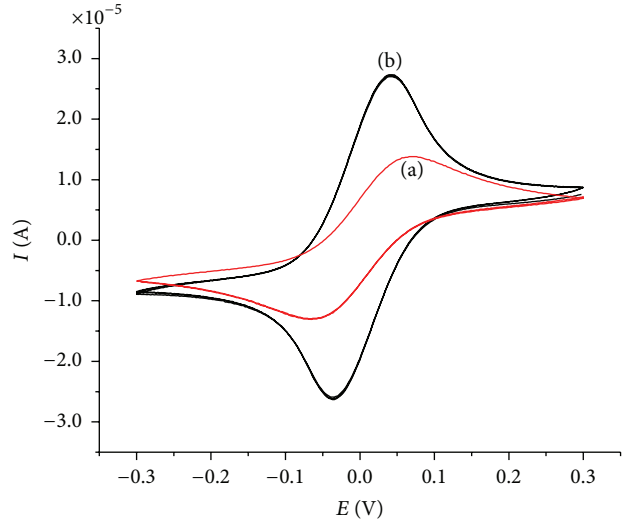

(a) WE: Pt
(b) WE: Pt/PPy NWs

Figure 8: Cyclic voltammograms measured in 0.03 M $K_3Fe(CN)_6/K_4Fe(CN)_6$ and 0.1 M KCl solution at 25 mV/s scan rate of the integrated three-electrode system inside the microchamber (a) before and (b) after electrochemical synthesis of PPy NWs on the working electrode.

a semicircle that characterizes charge transfer process and a linear region that characterizes diffusion process. This result further confirms that PPy NWs were formed on the electrode surface.

Cyclic Voltammograms of Pt and Pt/PPy NW Electrodes. Figure 8 shows the CV measured in 0.03 M $K_3Fe(CN)_6/K_4Fe(CN)_6$ and 0.1 M KCl solution at 25 mV/s scan rate of the integrated three-electrode system inside the microchamber before and after the electrochemical synthesis of PPy NWs. The potentials corresponding to the oxidation of Fe^{2+} and reduction of Fe^{3+} do not change. This result demonstrates that PPy NWs material formed on the working electrode has stable electrochemical behavior. Moreover, in the case of Pt/PPy NW working electrode (Figure 8(b)), the peak current is higher than that of Pt working electrode (Figure 8(a)). This observation is explained by the increase in specific surface area, thereby leading to the accumulation of the electroactive species on the surface, as well as the current density.

3.3. Determination of DNA Hybridization. When about 4 μL of sample containing 2 nM complementary target DNA was pumped into the microchamber, the DNA hybridization occurred rapidly; the response time was only few seconds and represented by the change in output signal (Figure 9(a)). We repeated the injection of a volume containing 2 nM noncomplementary target DNA; the output signal almost remained unchanged and was stable after one minute (Figure 9(b)).

The different concentrations of the target were tested with the microfluidics-based biosensor. The output signals increase linearly with the DNA target concentration and

Table 1: Comparison of the DNA sensor with some other works.

Technique of detection	Surface modification	Measurement system	Limit of detection	Reference
EIS	PPy NWs	Open system	10 pM	[20]
Lock-in amplifier	MWCNTs	Open system	1 nM	[23]
Lock-in amplifier	PPy NWs	Open system	100 pM	[21]
Electrochemical method	PPy film-AuNPs	Open system	150 pM	[24]
Lock-in amplifier	PPy NWs	Sealed system	20 pM	Current work

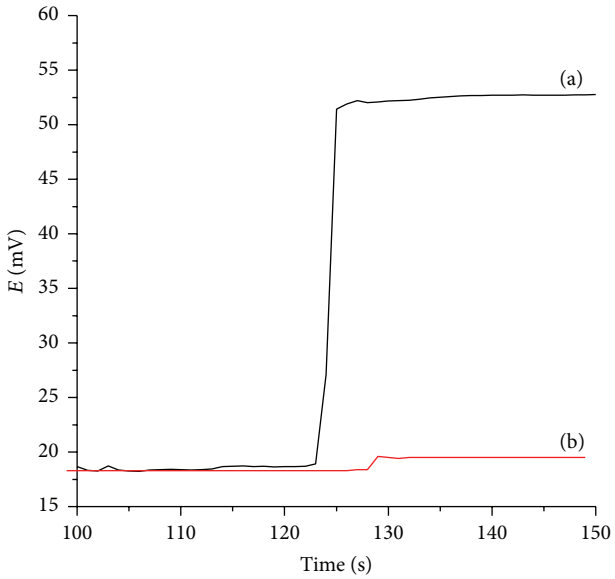

(a) 2 nM complementary DNA
(b) 2 nM noncomplementary DNA

Figure 9: The signals of DNA hybridization, $C_{\text{DNA probe}} = 10\,\mu$M, $T = 298$ K: (a) 2 nM complementary target DNA and (b) 2 nM noncomplementary target DNA.

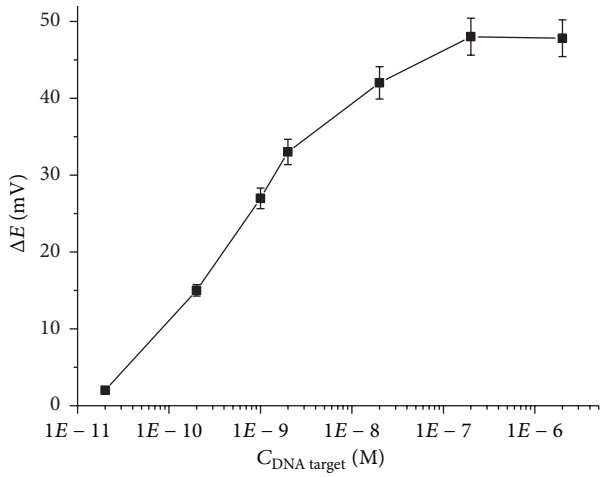

Figure 10: The signals of DNA hybridization corresponding to complementary target DNA with different concentrations.

reach the saturated value at $2{\cdot}10^{-7}$ M. The empirical data showed a detection limit of 20 pM (Figure 10). Table 1 shows that the obtained results in this work are much better than in our previous work [21] that used a similar detection method in an open system. The obtained results in this study are interesting because the fabrication processes for both electrodes and microchamber are simple (they do not require many photomasks or high-end etching machines); meanwhile, the limit of detection is comparable with other works. The injection volume is also much smaller than that required for the measurement in an open system. Performing measurements in the sealed microchamber could reduce possible noise and improve the response time.

4. Conclusion

We developed a platform consisting of an integrated three-electrode configuration fabricated with sputtering method and a PDMS-based microchamber. The PPy NWs were in situ synthesized in the sealed system at desired position using electrochemical method. The growth mechanism of PPy NWs in the presence of gelatin was investigated and proposed. DNA probe sequences were effectively immobilized on the surface of the DNA sensor through linkages with polypyrrole nanowires. DNA sensor can respond until the 20 pM addition of the target DNA into the microchamber at 25°C, which is greater than that reported previously in an open system under similar conditions. Moreover, the volume of the analytical sample was reduced when using the DNA sensor integrated with the microchamber compared with that in the open measuring cell. These results show that this simple and low-cost microfluidic platform has potential application for lab-on-chip electroanalytical device, in which the working electrode can be modified with conducting polymer in the microchamber.

Conflict of Interests

The authors declare that there is no conflict of interests regarding the publication of this paper.

Acknowledgment

This research is supported by the Vietnam National Foundation for Science and Technology Development (NAFOSTED) under Grant no. 103.02-2012.78.

References

[1] P. Tabeling, *Introduction to Microfluidics*, Oxford University Press, Oxford, UK, 2010.

[2] Y. Wang, Q. He, Y. Dong, and H. Chen, "In-channel modification of biosensor electrodes integrated on a polycarbonate microfluidic chip for micro flow-injection amperometric determination of glucose," *Sensors and Actuators, B: Chemical*, vol. 145, no. 1, pp. 553–560, 2010.

[3] H. Baccar, M. B. Mejri, R. Prehn et al., "Interdigitated microelectrode arrays integrated in microfluidic cell for biosensor applications," *Journal of Nanomedicine & Nanotechnology*, vol. 5, no. 6, article 243, 2014.

[4] J. Wu, R. Wang, H. Yu et al., "Inkjet-printed microelectrodes on PDMS as biosensors for functionalized microfluidic systems," *Lab on a Chip*, vol. 15, no. 3, pp. 690–695, 2015.

[5] S. Choi, M. Goryll, L. Y. M. Sin, P. K. Wong, and J. Chae, "Microfluidic-based biosensors toward point-of-care detection of nucleic acids and proteins," *Microfluidics and Nanofluidics*, vol. 10, no. 2, pp. 231–247, 2010.

[6] S. Prakash, M. Pinti, and B. Bhushan, "Theory, fabrication and applications of microfluidic and nanofluidic biosensors," *Philosophical Transactions of the Royal Society A: Mathematical, Physical and Engineering Sciences*, vol. 370, no. 1967, pp. 2269–2303, 2012.

[7] Y.-J. Yoon, K. H. H. Li, Y. Z. Low, J. Yoon, and S. H. Ng, "Microfluidics biosensor chip with integrated screen-printed electrodes for amperometric detection of nerve agent," *Sensors and Actuators, B: Chemical*, vol. 198, pp. 233–238, 2014.

[8] P. Neužil, S. Giselbrecht, K. Länge, T. J. Huang, and A. Manz, "Revisiting lab-on-a-chip technology for drug discovery," *Nature Reviews Drug Discovery*, vol. 11, no. 8, pp. 620–632, 2012.

[9] Z. Nie, C. A. Nijhuis, J. Gong et al., "Electrochemical sensing in paper-based microfluidic devices," *Lab on a Chip*, vol. 10, no. 4, pp. 477–483, 2010.

[10] N. M. M. Pires, T. Dong, U. Hanke, and N. Hoivik, "Recent developments in optical detection technologies in lab-on-a-chip devices for biosensing applications," *Sensors*, vol. 14, no. 8, pp. 15458–15479, 2014.

[11] K. N. Han, C. A. Li, M.-P. N. Bui et al., "On-chip electrochemical detection of bio/chemical molecule by nanostructures fabricated in a microfluidic channel," *Sensors and Actuators, B: Chemical*, vol. 177, pp. 472–477, 2013.

[12] S. K. Srivastava, R. Ramaneti, M. Roelse et al., "A generic microfluidic biosensor of G protein-coupled receptor activation—impedance measurements of reversible morphological changes of reverse transfected HEK293 cells on microelectrodes," *RSC Advances* , vol. 5, no. 65, pp. 52563–52570, 2015.

[13] H. E. A. Ferreira, D. Daniel, M. Bertotti, and E. M. Richter, "A novel disposable electrochemical microcell: construction and characterization," *Journal of the Brazilian Chemical Society*, vol. 19, no. 8, pp. 1538–1545, 2008.

[14] R. A. B. da Silva, E. G. N. de Almeida, A. C. Rabelo, A. T. C. da Silva, L. F. Ferreira, and E. M. Richter, "Three electrode electrochemical microfluidic cell: construction and characterization," *Journal of the Brazilian Chemical Society*, vol. 20, no. 7, pp. 1235–1241, 2009.

[15] J. Puigmartí-Luis, M. Rubio-Martínez, U. Hartfelder, I. Imaz, D. Maspoch, and P. S. Dittrich, "Coordination polymer nanofibers generated by microfluidic synthesis," *Journal of the American Chemical Society*, vol. 133, no. 12, pp. 4216–4219, 2011.

[16] M. Y. Elahi, S. Z. Bathaie, S. H. Kazemi, and M. F. Mousavi, "DNA immobilization on a polypyrrole nanofiber modified electrode and its interaction with salicylic acid/aspirin," *Analytical Biochemistry*, vol. 411, no. 2, pp. 176–184, 2011.

[17] M. Gerard, A. Chaubey, and B. D. Malhotra, "Application of conducting polymers to biosensors," *Biosensors and Bioelectronics*, vol. 17, no. 5, pp. 345–359, 2002.

[18] W. Wernet, "Thermoplastic and elastic conducting polypyrrole films," *Synthetic Metals*, vol. 41, no. 3, pp. 843–848, 1991.

[19] J. Kochana, K. Hnida, G. Sulka, P. Knihnicki, J. Kozak, and A. Gilowska, "Application of polypyrrole nanowires for the development of a tyrosinase biosensor," *Chemical Papers*, vol. 69, no. 8, pp. 1130–1135, 2015.

[20] T. L. Tran, T. X. Chu, D. C. Huynh, D. T. Pham, T. H. T. Luu, and A. T. Mai, "Effective immobilization of DNA for development of polypyrrole nanowires based biosensor," *Applied Surface Science*, vol. 314, pp. 260–265, 2014.

[21] A. T. Mai, T. P. Duc, X. C. Thi, M. H. Nguyen, and H. H. Nguyen, "Highly sensitive DNA sensor based on polypyrrole nanowire," *Applied Surface Science*, vol. 309, pp. 285–289, 2014.

[22] J. Jang, "Conducting polymer nanomaterials and their applications," in *Emissive Materials Nanomaterials*, vol. 199 of *Advances in Polymer Science*, pp. 189–260, Springer, Berlin, Germany, 2006.

[23] N. T. Thuy, P. D. Tam, M. A. Tuan et al., "Detection of pathogenic microorganisms using biosensor based on multi-walled carbon nanotubes dispersed in DNA solution," *Current Applied Physics*, vol. 12, no. 6, pp. 1553–1560, 2012.

[24] E. Spain, T. E. Keyes, and R. J. Forster, "Polypyrrole-gold nanoparticle composites for highly sensitive DNA detection," *Electrochimica Acta*, vol. 109, pp. 102–109, 2013.

[25] L. T. H. Thuong, T. T. Luyen, D. P. Quan et al., "Design and fabrication of microfluidic biosensor composed of a PDMS microchannel and three electrode platform for electrochemical measurement," in *Proceedings of the 2nd International Conference on Advanced Materials and Nanotechnology (ICAMN '14)*, pp. 254–260, Hanoi, Vietnam, October-November 2014.

[26] D. Ge, J. Mu, S. Huang et al., "Electrochemical synthesis of polypyrrole nanowires in the presence of gelatin," *Synthetic Metals*, vol. 161, no. 1-2, pp. 166–172, 2011.